Supporting Information for

Oligomeric Poly(acetalcarbonates) Obtained by Repolymerisation of Paraformaldehyde

Claudia Bizzarri, Henning Vogt, Gábor Baráth, Christoph Gürtler, Walter Leitner and Thomas E. Müller

Table of content

1. ^{1}H, ^{13}C, and HMBC NMR spectra of compounds **H** and **A**
2. Mass spectroscopic analysis
3. Thermal analysis
4. Synthesis of hydroxyl-terminated poly(acetalcarbonate) **H** with ^{13}C-labelled CO_2

1. ^{1}H, ^{13}C, and HMBC NMR spectra of compounds H and A

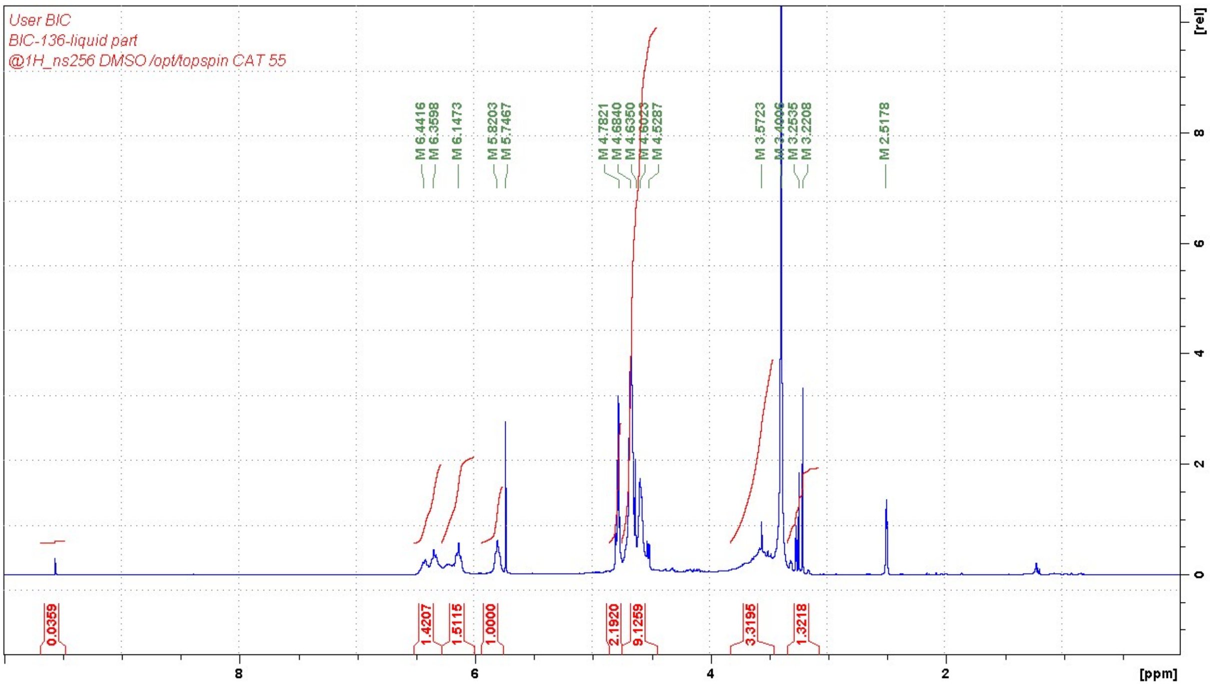

Figure S1. ^{1}H NMR spectrum of compound **H** in *d6*-DMSO (residual solvent signal: 2.5 ppm; water signal: 3.4 ppm).

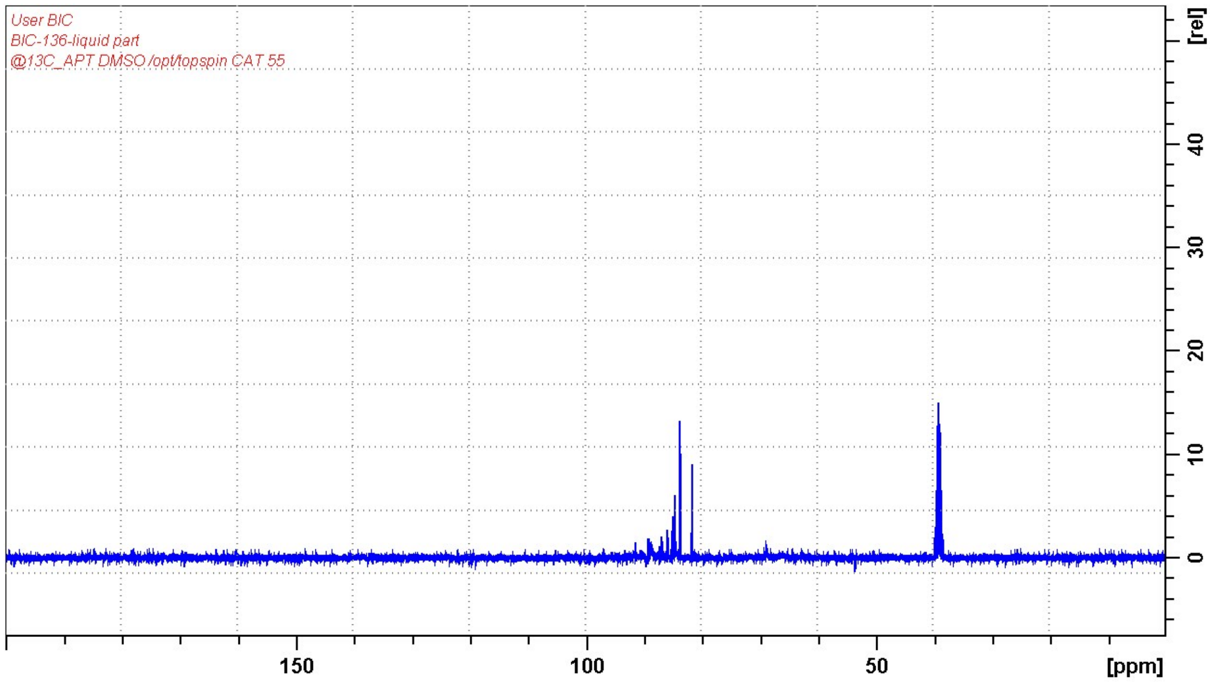

Figure S2. ^{13}C NMR spectrum of compound **H** in *d6*-DMSO (solvent signal: 39.5 ppm).

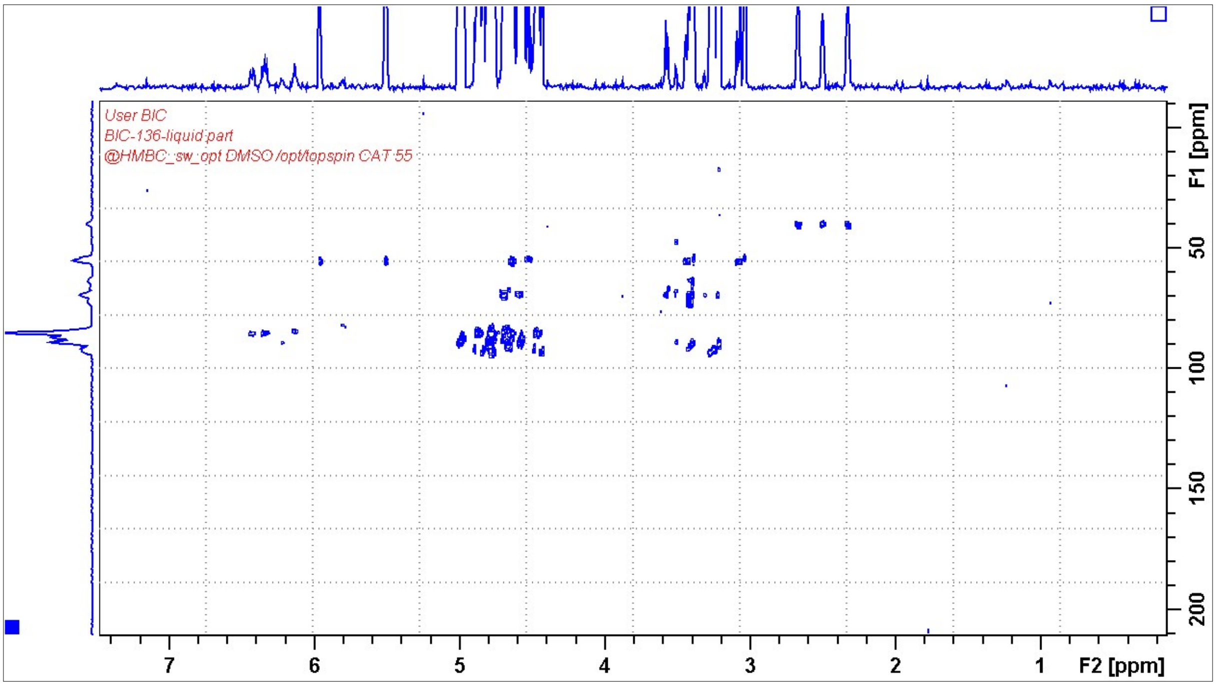

Figure S3. HMBC spectrum of compound **H** in *d6*-DMSO (^{1}H residual solvent signal: 2.5 ppm; ^{13}C solvent signal: 39.5 ppm; ^{1}H water signal: 3.4 ppm).

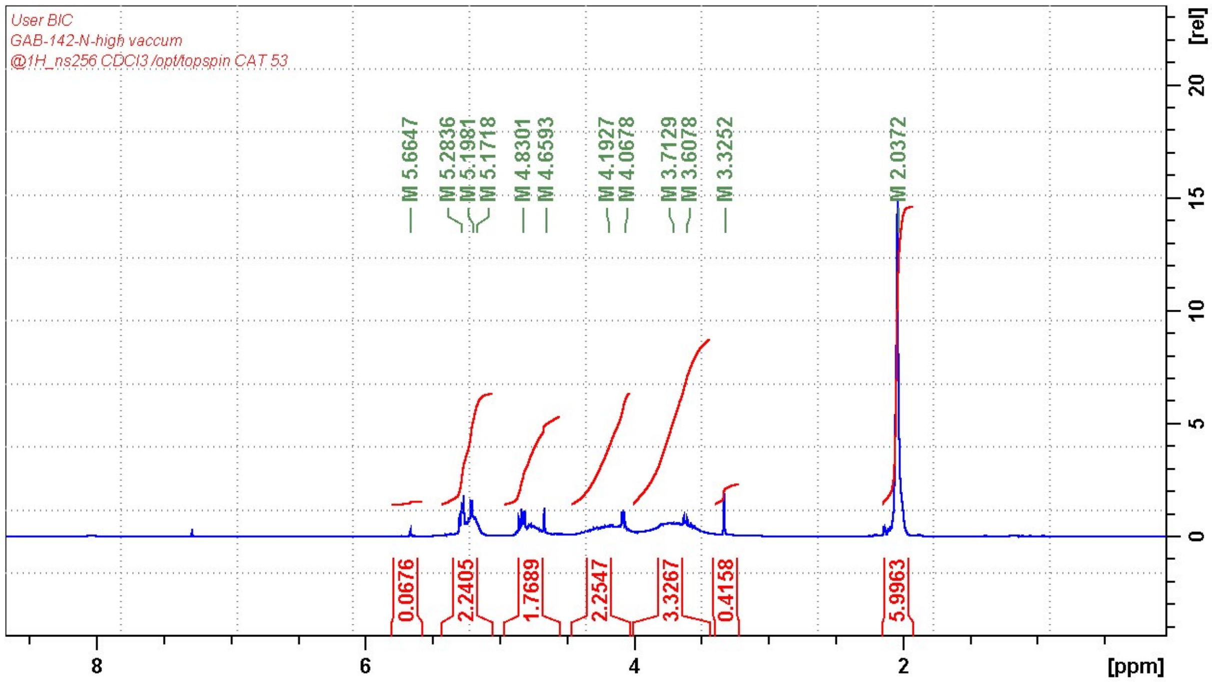

Figure S4. ^{1}H NMR spectrum of compound **A** in $CDCl_3$ (residual solvent signal: 7.26 ppm).

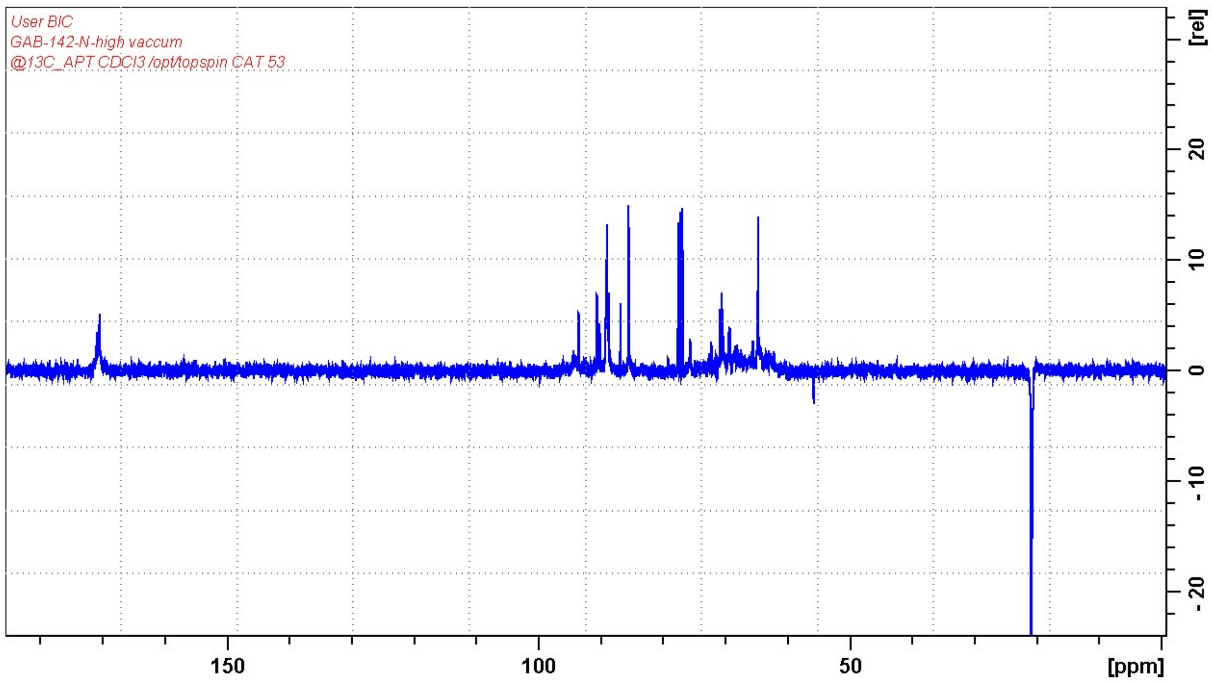

Figure S5. ^{13}C NMR spectrum of compound **A** in $CDCl_3$ (solvent signal: 77 ppm).

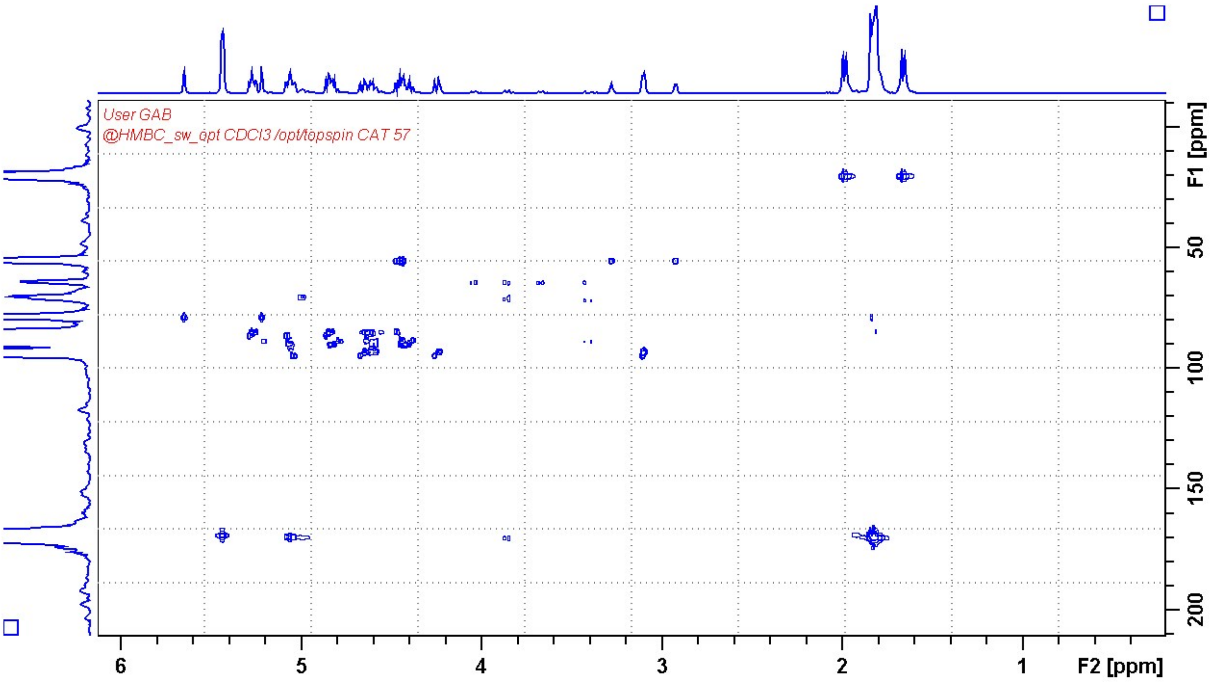

Figure S6. HMBC spectrum of compound **A** in $CDCl_3$ (solvent signal: 77 ppm).

2. Mass spectroscopic analysis

2.1. ESI-MS spectroscopy

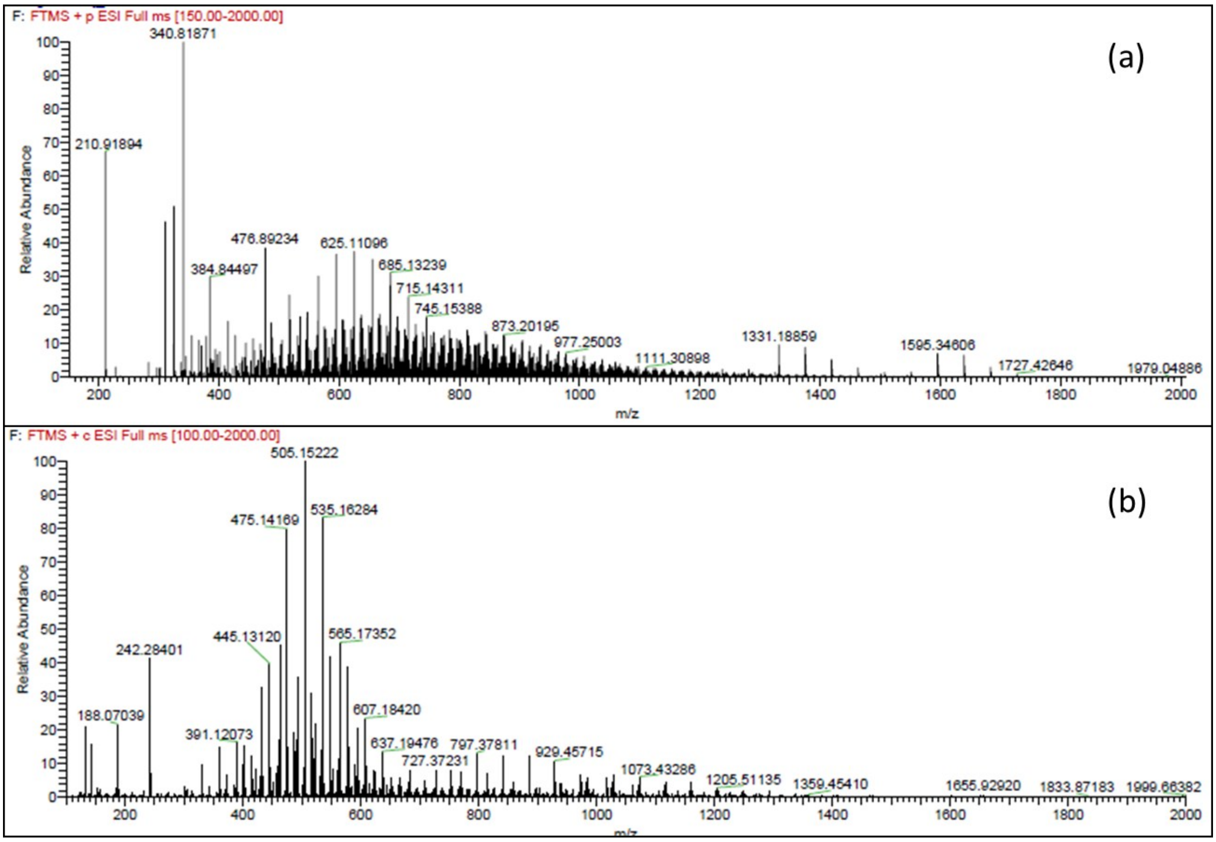

Figure S7. High-resolution electron spray mass spectra (ESI-MS) confirming the oligomeric nature of compounds **H** (top) and **A** (bottom).

2.2. MALDI-TOF analysis

General sum formula **H**: $[HO(CH_2O)_n(CO_2)_o(CH_2CH_2O)_mH]^+ \rightarrow [(FA)_n(CO_2)_o(EO)_m]$

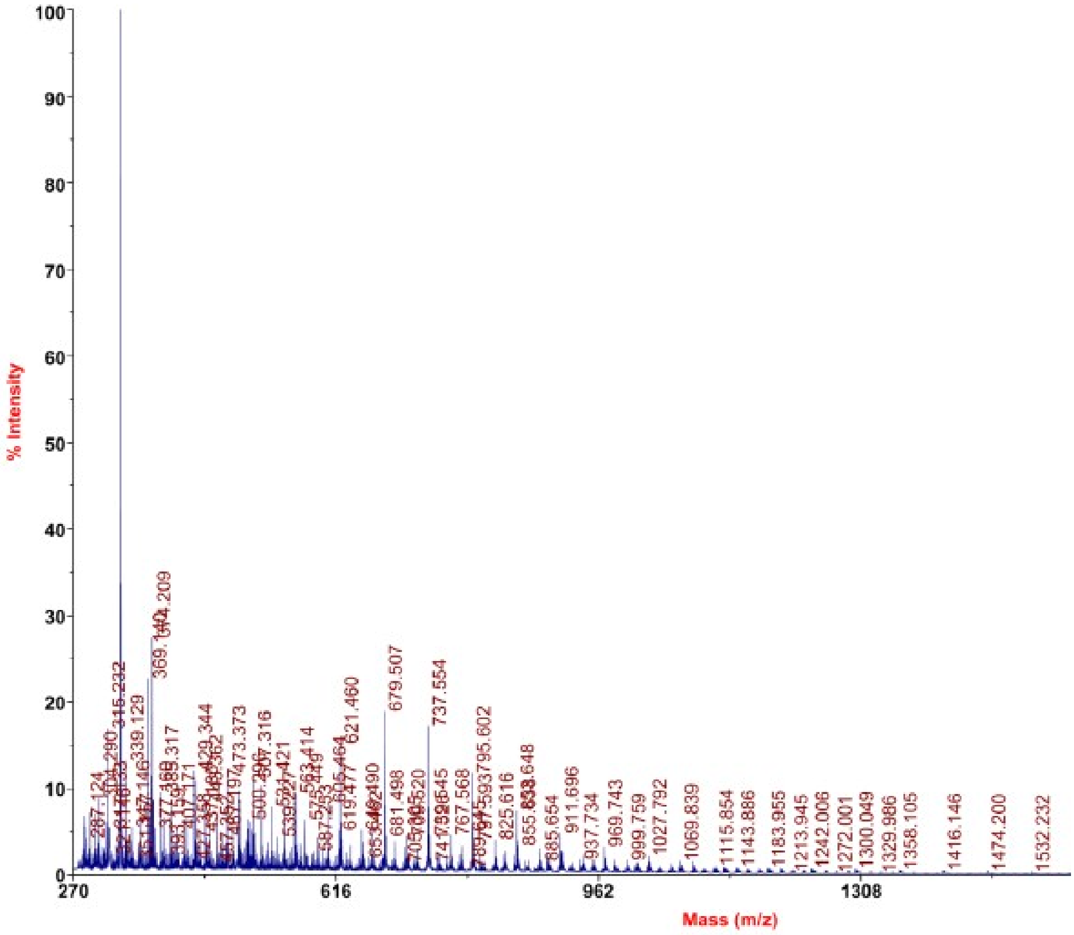

Figure S8. Matrix assisted Laser Desorption Ionization (MALDI-TOF) spectrum of product **H.** (Δ m/z = 58.04 $\rightarrow$ +2 EO -1FA)

Table S1. Analysis of the MALDI-TOF series of compound **H**

	Series 1 $[(FA)_n(EO)_m(CO_2)_o]^+$		**Series 1a** $[(FA)_n(EO)_m(CO_2)_{(o+1)}]^+$		**Series 1b** $[(FA)_n(EO)_{(m+1)}(CO_2)_{(o+1)}]^+$	
	m/z	**Rel. intensity**	**m/z**	**Rel. intensity**	**m/z**	**Rel. intensity**
	283.13	2.91	327.12	3.00		
+ 1 FA unit	313.14	3.71	357.13	3.19		
"	343.15	3.85	387.15	2.61		
"	373.16	3.88	417.16	2.36	461.21	1.72
"	403.18	3.52	447.17	2.24	491.21	1.57
"	433.19	3.30	477.19	2.25	521.22	1.37
"	463.20	2.74			581.25	1.15
"	493.22	2.49	537.22	1.88	611.27	1.04
"	523.23	2.21	567.23	1.71		
"	553.24	1.92	597.25	1.46		
"	583.29	1.72	627.26	1.32		
"	613.27	1.45	657.28	1.32		
"	643.28	1.28	687.30	1.08		
"	673.31	1.07	717.31	0.99		
	Series 2 $[(FA)_n(EO)_m(CO_2)_o]^+$		**Series 2a** $[(FA)_n(EO)_m(CO_2)_{(o+1)}]^+$		**Series 2b** $[(FA)_n(EO)_{(m+1)}(CO_2)_{(o+1)}]^+$	
	m/z	**Rel. intensity**	**m/z**	**Rel. intensity**	**m/z**	**Rel. intensity**
+1FA unit					289.13	2.37
"					319.14	2.77
"			305.13	3.14	349.15	2.57
"	291.14	2.99	335.15	3.15	379.17	2.57
"	321.15	2.33	365.16	2.58	409.18	2.56
"	351.16	1.75	395.17	2.41	439.20	2.54
"	381.18	1.29	425.18	2.11	469.21	2.29
"			455.20	1.85		
"			485.21	1.70	529.24	1.92
"			515.22	1.46	559.25	1.77
"			545.24	1.3	589.26	1.59
"					619.48	5.04
"					649.5	5.10
"					679.51	18.34
"					709.52	4.39
"					739.54	4.55
"					769.56	2.04
"					799.57	1.61
"					829.59	0.97
	Series 3 $[(FA)_n(EO)_m(CO_2)_o]^+$		**Series 3a** $[(FA)_n(EO)_m(CO_2)_{(o+1)}]^+$			
	m/z	**Rel. intensity**	**m/z**	**Rel. intensity**		

+1FA unit	331.18	3.64				
"	361.17	3.01	405.16	3.57		
"	391.17	2.99	435.18	3.43		
"	421.19	2.91	465.19	3.19		
"	451.20	2.77	495.20	3.07		
"	481.21	2.81	525.22	2.83		
"	511.23	2.41	555.23	2.65		
"	541.24	2.34	585.24	2.43		
"	571.25	2.13	615.26	2.13		
"	601.27	1.85	645.28	1.92		
"	631.28	1.66	675.29	1.67		
"	661.30	1.45	705.31	1.34		
"	691.31	1.25	735.32	1.32		
"	721.33	1.16	765.33	1.1		
"	751.34	0.98				
	Series 4 $[(FA)_n(EO)_m(CO_2)_o]^+$		**Series 4a $[(FA)_n(EO)_{(m+1)}(CO_2)_{(o)}]^+$**		**Series 4b $[(FA)_n(EO)_{(m+2)}(CO_2)]^+$**	
	m/z	**Rel. intensity**	**m/z**	**Rel. intensity**	**m/z**	**Rel. intensity**
+1FA unit	355.30	3.66			487.39	9.67
"	385.32	9.53			517.40	10.01
"	415.32	6.43	503.38	6.08	547.42	7.99
"	445.31	3.09	533.38	2.19	577.43	2.11
"	475.33	2.05	563.41	9.16	607.45	1.91
"	505.37	5.21	593.43	2.74	637.45	1.20
"	535.39	2.70	623.45	4.12		
"			653.46	1.96		
"			683.48	1.30		
	Series 5 $[(FA)_n(EO)_m(CO_2)_o]^+$		**Series 5a $[(FA)_n(EO)_{(m+1)}(CO_2)_{(o)}]^+$**		**Series 5b $[(FA)_n(EO)_{(m+1)}(CO_2)_{(o+1)}]^+$**	
+1FA unit					287.12	4.25
"					317.13	5.38
"					347.15	5.44
"	289.13	2.37	337.15	1.93	377.16	5.37
"	319.14	2.77	363.15	2.67	407.17	5.33
"	349.15	2.66	393.16	2.32	437.18	4.97
"	379.17	2.57	423.18	2.15	467.20	4.57
"	409.18	2.56	453.19	1.82	497.21	4.08
"	439.20	2.54	483.21	1.66	527.23	3.64
"	469.22	2.29	513.25	1.45	557.24	3.12
	Series 5 $[(FA)_n(EO)_m(CO_2)_o]^+$		**Series 5a $[(FA)_n(EO)_{(m+1)}(CO_2)_{(o)}]^+$**		**Series 5b $[(FA)_n(EO)_{(m+1)}(CO_2)_{(o+1)}]^+$**	
+1FA unit	283.23	2.03				
"	313.24	6.08				
"	343.23	2.27				
"	373.28	11.41				

General sum formula of compound **A**:

$[H_3CC(O)O(CH_2O)n(CO_2)o(CH_2CH_2O)_mC(O)CH_3]^+ \rightarrow [(FA)_n(CO_2)_o(EO)_m]$

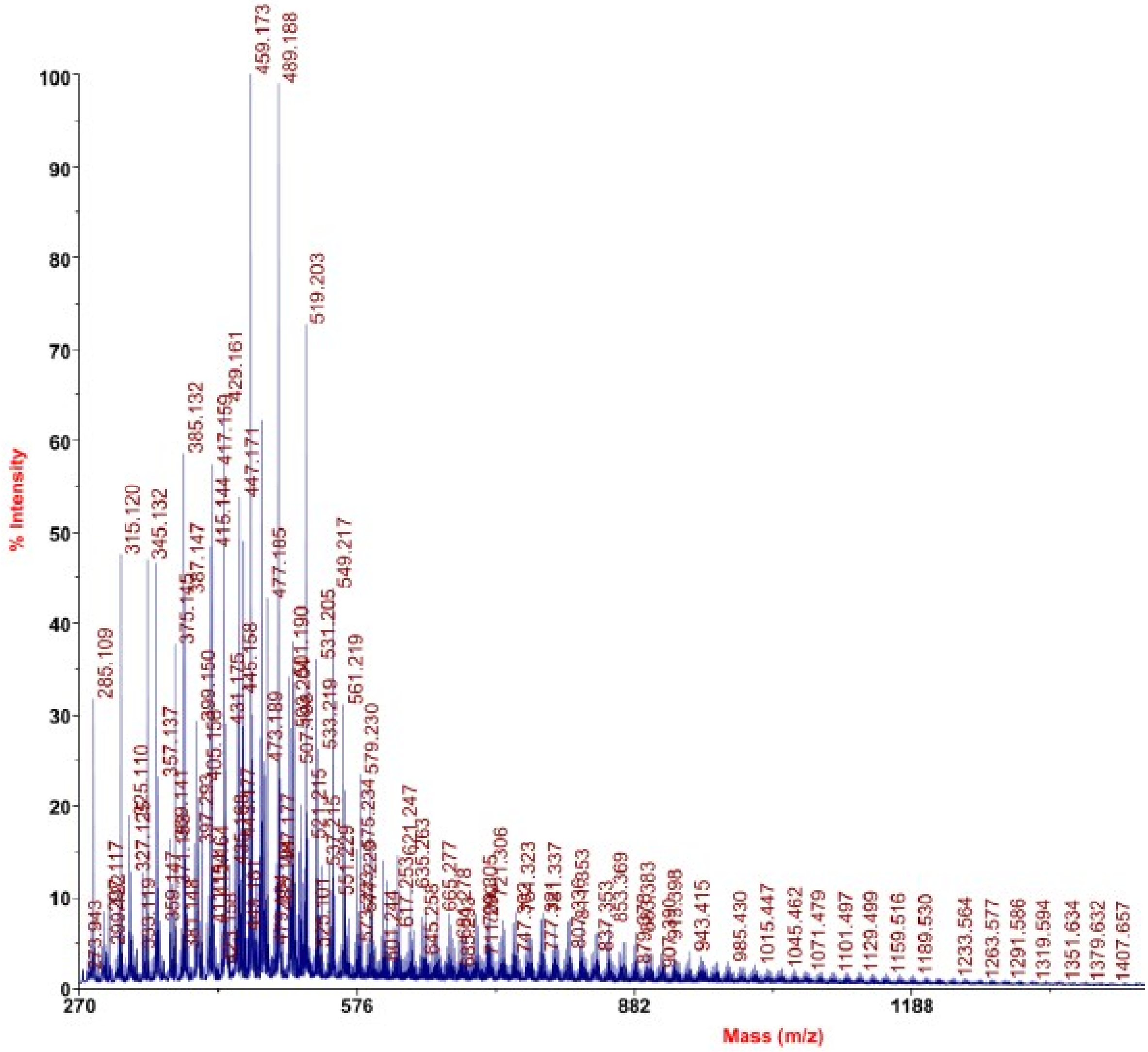

Figure S9. Matrix Assisted Laser Desorption Ionization (MALDI-TOF) spectrum of product **A.**

Table S2. Assignment of the MALDI-TOF series in compound **A**

	Series 1 $[(FA)_n(EO)_m(CO_2)_o]^+$		**Series 1a** $[(FA)_n(EO)_m(CO_2)_{(o+1)}]^+$		**Series 1b** $[(FA)_n(EO)_{(m+1)}(CO_2)_{(o+1)}]^+$	
	m/z	**Rel. intensity**	**m/z**	**Rel. intensity**	**m/z**	**Rel. intensity**
	281.11	2.84	325.11	18.87	369.14	16.33
+ 1 FA unit	311.13	3.71	355.12	46.26	399.15	29.02
"	341.14	5.81	385.13	58.03	429.16	63.57
"	371.15	11.3	415.14	47.75	459.17	98.99
"	401.16	20.8	445.16	31.96	489.19	97.88
"	431.18	28.69	475.17	23.15	519.20	69.08
"	461.19	29.69	505.19	13.52	549.22	41.71
"	491.20	22.76	535.21	8.18	579.23	22.44
"	521.22	15.74	565.23	5.78	609.24	11.34
"	551.23	9.80	595.25	4.31	639.26	6.21
"	581.24	6.04	625.26	3.23	669.27	3.51
"	611.26	3.85	655.28	2.78	699.30	2.56
"	641.27	2.97	685.29	2.38	729.30	1.92
"	701.28	2.71	715.29	3.02	759.32	1.79
"	731.30	3.06	745.31	2.54	789.33	2.01
"	761.31	3.70	775.33	2.85	819.35	4.68
"	791.33	4.24	805.34	3.14	849.36	2.21
"	821.34	4.68	835.36	3.75	879.38	2.71
"	851.36	4.88	865.37	4.00	909.39	2.57
"	881.37	4.70	895.39	4.03	939.41	2.67
"	911.39	3.87	925.40	3.90	969.42	2.41
"	941.40	3.06	955.42	3.48	999.44	2.23
"	971.42	2.75				
"	1001.44	2.20				
	Series 2 $[(FA)_n(EO)_m(CO_2)_o]^+$		**Series 2a** $[(FA)_n(EO)_m(CO_2)_{(o+1)}]^+$		**Series 2b** $[(FA)_n(EO)_{(m+1)}(CO_2)_{(o+1)}]^+$	
	m/z	**Rel. intensity**	**m/z**	**Rel. intensity**	**m/z**	**Rel. intensity**
			315.12	47.15	359.15	7.33
"			345.13	46.51	389.16	8.16
"			375.14	37.31	419.17	7.01
"			405.16	22.63	449.18	6.4
"			435.17	13.42	479.19	4.85
"			495.20	5.99	509.21	3.83
"			525.20	4.16	539.22	2.85
"			555.22	2.88	569.23	2.69
"	541.22	2.0	585.23	2.55	599.25	2.94
"	571.25	2.40	615.24	2.99	629.25	3.45
"	601.24	3.10	645.26	3.72	659.27	3.85
"	631.26	3.99	675.24	4.51	689.28	5.21
"	661.28	5.01	705.28	5.51	719.30	7.00

"	691.29	6.13	735.30	5.66	749.31	6.93
"	721.31	9.77	765.32	5.44	779.32	7.33
"	751.32	8.16	795.34	4.87	809.34	7.04
"	781.34	8.04	825.35	4.17	839.35	5.85
"	811.35	7.35	855.37	3.89	869.37	4.96
"	841.37	6.15	885.39	3.21	899.38	3.84
"	871.38	4.91	915.41	2.78	829.40	2.9
"	901.40	3.74	945.42	2.02	959.41	2.56
"	931.41	2.85	975.44	1.67	989.44	1.67
"	961.42	2.13	1005.45	1.55		
"	991.44	1.75				
	Series 3 **$[(FA)_n(EO)_m(CO_2)_o]^+$**		**Series 3a** **$[(FA)_n(EO)_m(CO_2)_{(o+1)}]^+$**		**Series 3b** **$[(FA)_n(EO)_{m+1}(CO_2)_{(o)}]^+$**	
	m/z	**Rel. intensity**	**m/z**	**Rel. intensity**	**m/z**	**Rel. intensity**
	291.12	4.18	305.11	2.11		
"	321.12	3.45	335.11	1.69		
"	351.14	3.33			395.16	2.28
"	381.15	4.33			425.17	3.13
"	411.15	7.13			455.18	5.54
"	441.16	14.69			485.19	8.55
"	471.17	61.59			515.21	11.10
"	501.19	33.77			545.22	13.48
"	531.20	34.64			575.23	14.73
"	561.22	29.68			605.25	13.44
"	591.23	21.52			635.26	10.68
"	621.25	13.95			665.28	8.17
"	651.26	8.43			695.29	5.96
"	681.28	5.34			725.31	4.41
"	711.30	3.62			755.32	3.16
"	741.32	2.69			785.33	2.55
"	771.33	2.05	815.36	1.92		
"	801.35	1.85	845.36	1.62		
"	831.36	1.68	875.38	1.55		
"	861.38	1.44	905.38	1.38		
"	891.38	1.49	935.40	1.46		
"	921.40	1.50	965.41	1.76		
"	951.41	1.87	995.43	1.67		
"	981.43	1.75				
"	1011.45	1.77				
	Series 4 = Series 1b **$[(FA)_n(EO)_m(CO_2)_o]^+$**		**Series 4a** **$[(FA)_n(EO)_m(CO_2)_{(o+1)}]^+$**		**Series 4b** **$[(FA)_n(EO)_m(CO_2)_{(o+2)}]^+$**	
	m/z	**Rel. intensity**	**m/z**	**Rel. intensity**	**m/z**	**Rel. intensity**
			293.13	1.75		
"	279.13	3.17	323.13	2.24	367.14	1.96
"	309.12	3.22	353.14	3.63	397.14	3.40

“	339.13	12.69	383.15	6.64	427.15	6.16
“	369.14	16.33	413.16	10.12	457.14	22.55
“	399.15	29.02	443.18	16.45	487.18	13.59
“	429.16	63.57	473.19	24.6	517.19	12.93
“	459.17	98.99	503.20	28.22	547.21	10.54
“	489.19	97.88	533.22	25.04	577.23	8.46
“	519.20	69.08	563.23	20.90	607.25	6.41
“	549.22	41.71	593.25	14.80	637.27	5.29
“	579.23	22.44	623.26	10.22	667.29	4.34
“	609.24	11.34	653.28	6.15	697.30	3.60
“	639.26	6.21	683.29	4.28	727.31	2.87
“	669.27	3.51	713.30	3.21	757.33	2.23
“	699.30	2.56	743.31	2.43	787.34	2.01
“	729.30	1.92	773.32	1.90	817.36	1.89
“	759.32	1.79	803.34	2.11	847.36	1.87
“	789.33	2.01	833.35	2.10	877.38	1.80
“	819.35	4.68	863.36	2.21	907.39	2.23
“	849.36	2.21	893.38	2.28	937.40	2.16
“	879.38	2.71	923.39	2.55	967.42	2.38
“	909.39	2.57	953.41	2.43	997.43	2.31
“	939.41	2.67	983.43	2.42		
“			1013.44	2.19		
	Series 5 **$[(FA)_n(EO)_m(CO_2)_o]^+$**		**Series 5a** **$[(FA)_n(EO)_m(CO_2)_{(o+1)}]^+$**		**Series 5b** **$[(FA)_n(EO)_m(CO_2)_{(o+2)}]^+$**	
	m/z	**Rel. intensity**	**m/z**	**Rel. intensity**	**m/z**	**Rel. intensity**
“			303.10	9.98		
“			333.12	4.37		
“			363.14	3.07		
“			393.15	2.33	437.16	1.95
“			423.16	2.77	467.16	2.44
“			453.14	5.58		
“	439.18	2.07	483.19	6.48		
“	469.15	14.44	513.20	---		
“	499.19	2.60	543.21	3.86		
“	529.21	3.64	573.22	4.95		
“	559.22	4.88	603.24	5.66		
“	589.24	5.71	633.25	6.07		
“	619.25	5.98	663.27	5.57		
“	649.28	6.71	693.28	5.22		
“	679.29	6.87	723.30	5.00		
“	709.30	6.75	753.32	4.01		
“	739.32	6.32	783.34	3.31		
“	769.34	5.26				
“	799.35	4.20				
“	829.37	3.19				
“	859.38	2.50				

"	889.39	1.97				
"	919.40	1.50				
"	949.41	1.52				
	Series 6 = Series 2b $[(FA)_n(EO)_m(CO_2)_o]^+$		**Series 6a $[(FA)_n(EO)_m(CO_2)_{(o+1)}]^+$**			
			283.10	6.64		
"			313.11	10.84		
"			343.12	10.31		
"			373.13	8.67		
"	359.15	7.33	403.15	7.32		
"	389.16	8.16	433.16	6.18		
"	419.17	7.01	463.17	6.35		
"	449.18	6.40	493.20	4.08		
"	479.19	4.85	523.22	3.27		
"	509.21	3.83	553.23	2.59		
"	539.22	2.85	583.24	2.18		
"	569.23	2.69	613.26	2.26		
"	599.25	2.94	643.27	2.37		
"	629.25	3.45	673.28	2.97		
"	659.27	3.85	703.29	3.78		
"	689.28	5.21	733.31	4.98		
"	719.30	7.00	763.32	5.83		
"	749.31	6.93	793.34	6.72		
"	779.32	7.33	823.35	7.20		
"	809.34	7.04	853.37	7.11		
"	839.35	5.85	883.38	6.02		
"	869.37	4.96	913.40	5.22		
"	899.38	3.84	943.42	4.06		
"	829.40	2.90	973.43	2.93		
"	959.41	2.56	1003.44	2.15		
	989.44	1.67				
	Series 8 $[(FA)_n(EO)_m(CO_2)_o]^+$		**Series 8a $[(FA)_n(EO)_m(CO_2)_{(o+1)}]^+$**		**Series 8b $[(FA)_n(EO)_{(m+1)}(CO_2)_{(o+1)}]^+$**	
	m/z	**Rel. intensity**	**m/z**	**Rel. intensity**	**m/z**	**Rel. intensity**
"			354.12	4.67		
"	340.14	5.75	384.14	5.94	428.16	6.93
"	370.15	6.08			458.16	14.11
"					488.19	11.60
"					518.20	9.32

3. Thermal analysis

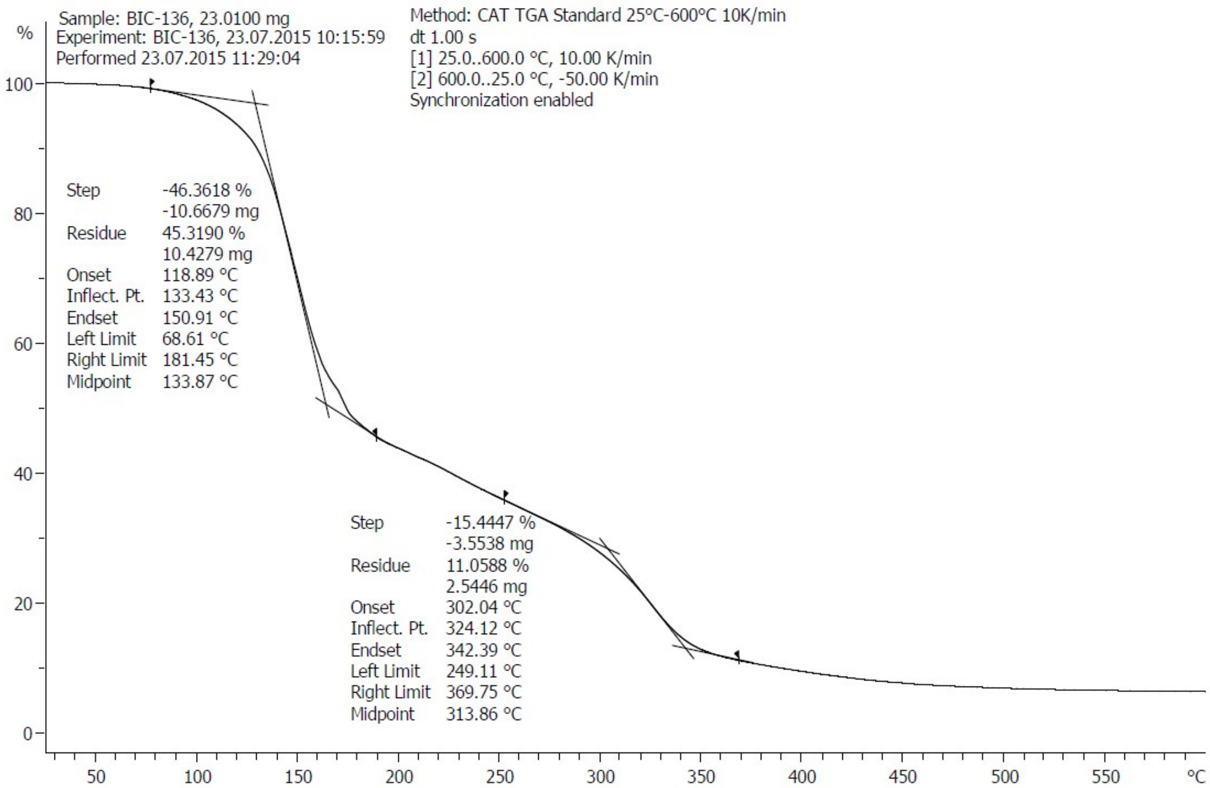

Figure S10. Thermogravimetric analysis of compound **H**. Two degradation steps can be recognized.

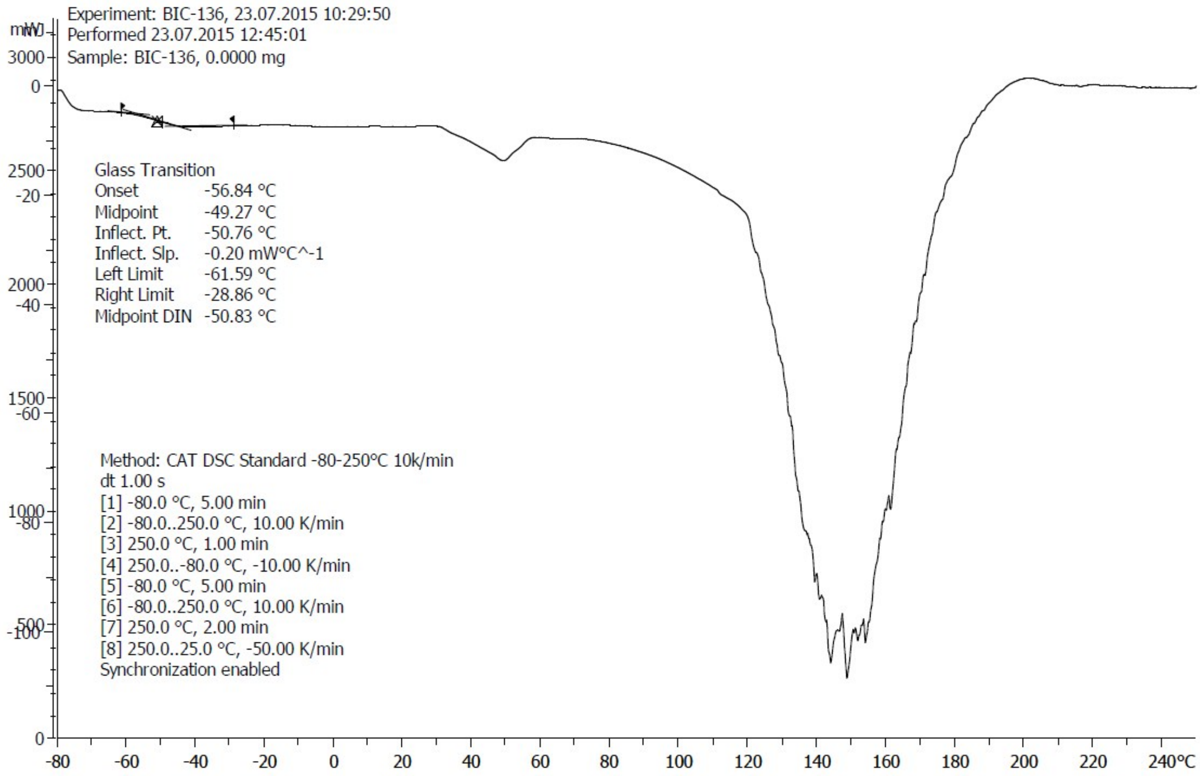

Figure S11. Differential scanning calorimetry trace of compound **H**. The glass transition temperature is at -50.8 °C.

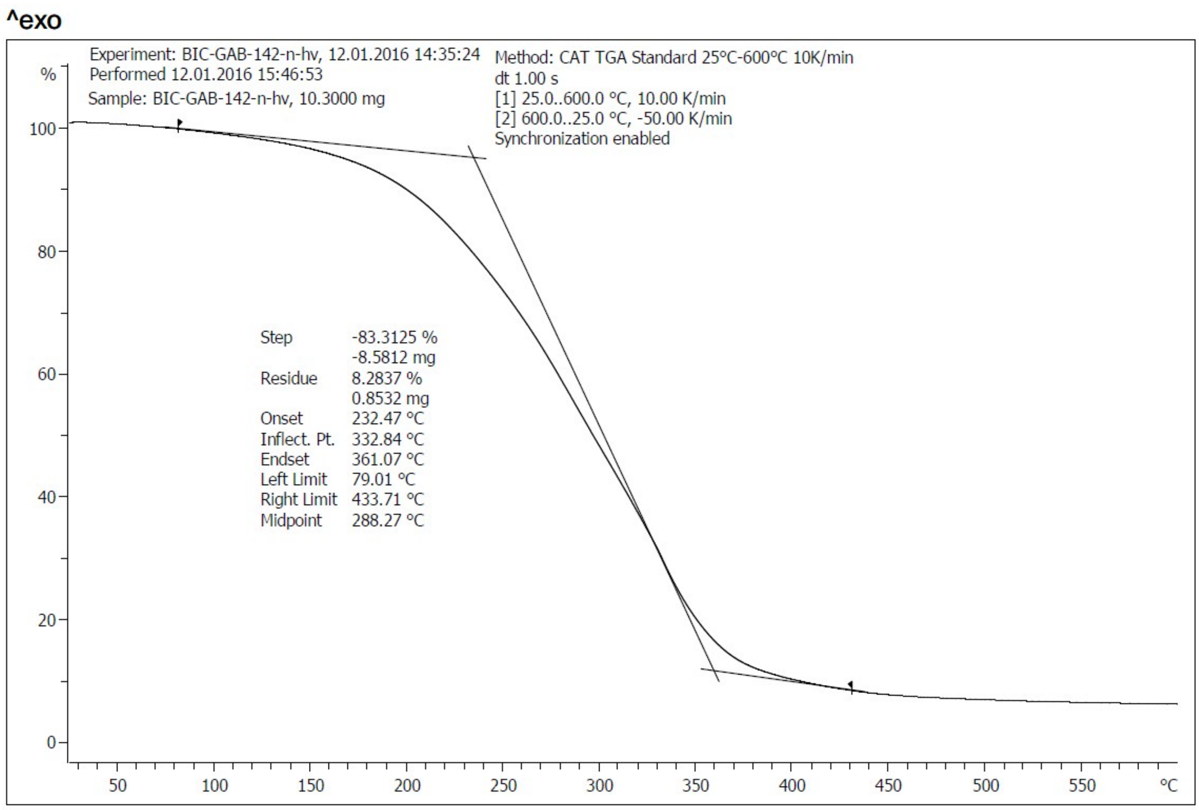

Figure S12. Thermogravimetric analysis of compound **A**.

To understand the effect of the choice of the Lewis acid catalyst, a series of compounds with the structure M(EtHex)$_n$, where M is a metal centre with valence *n* and EtHex is 2-ethylhexanoate, and Sn(OAc)$_2$ were tested under the same reaction conditions (Table S1).

Table S1. Screening of Lewis acid catalysts for the repolymerisation of paraformaldehyde

Sample	Lewis acid	M_n [g/mol]	PDI	FA units[a]	CO_2 / EO[a, b]
A	DBTL	644	1.23	10	3
A2	Cu(EtHex)$_2$	841	1.19	12	3
A3	Zn(EtHex)$_2$	645	1.09	11	3
A4	Sn(EtHex)$_2$	799	1.19	10	3
A5	Bi(EtHex)$_3$	648	1.19	10	3
A6	Sn(OAc)$_2$	639	1.08	10	3

DBTL, dibutyltinlaurate; EtHex, 2-ethylhexanoate;
[a] Composition of the oligomeric molecule assigned to the signal with the highest intensity in the mass spectra (ESI-MS); [b] Units of CO_2 and EO: x CO_2 + y EO; where x≥1 and y≥1 .

The thermal behaviour of the products was characterised by differential scanning calorimetry (DSC). The glass transition temperature was in the range from -65.5 °C to -42.7 °C (Table S3). The small variation in T_g may be related to the nature of the oligomeric chain, where the distribution of oxymethylene, oxyethylene, and carbonate units has different effects on the intermolecular forces, chain stiffness, and chain symmetry.

Table S3. Thermal stability, glass transition temperature (T_g) and viscosity (μ) of oligomeric poly(acetalcarbonates) obtained with different catalyst combinations.

Sample	Lewis acid	**Thermal stability** T_d [°C] (weight loss [%])		T_g [°C]	μ [Pa·s]
		1st Step	2nd Step		
H	DBTL	95 (23.4)	229 (23.1)	-56.8	13.42
A	DBTL	232 (96.0)	--	-63.1	0.29
A2	Cu(EtHex)$_2$	149 (83.2)	--	-60.1	--
A3	Zn(EtHex)$_2$	223 (74.0)	--	-65.5	--
A4	Sn(EtHex)$_2$	100 (2.54)	173 (40.4)	-58.8	--
A5	Bi(EtHex)$_3$	195 (48.2)	319 (7.2)	-42.7	--
A6	Sn(OAc)$_2$	153 (77.4)	--	-58.2	--

4. Synthesis of hydroxyl-terminated poly(acetalcarbonate) H with ^{13}C-labelled CO_2

The general procedure was repeated with ^{13}C labelled CO_2 using DBTL (12.4 mg, 0.020 mmol) as a Lewis acid and $CsCO_3$ (1.65 g, 5.06 mmol) as Lewis base and was carried out in dioxane. Labelled $^{13}CO_2$-gas was used for pressurizing the autoclave. Opening the autoclave revealed a colourless solution with a small amount of solid white particles. After complete work-up of the reaction mixture a colourless viscous liquid (6.31 g) was obtained.

GPC: A number-average molar mass of M_n = 655 g/mol and a polydispersity index of PDI = 1.22 was determined by GPC in chloroform.

^{1}H NMR spectroscopy (400 MHz, $CDCl_3$): δ = 2.02-2.07 (m, 1.00 H, CH_3), 3.32-3.35 (m, 0.29 H), 3.54-3.65 (m, 0.07 H), 4.06-4.11 (m, 0.02 H), 4.65-4.69 (m, 0.18 H, O-CH_2-O), 4.71 (s, 0.02 H, O-CH_2-O), 4.77-4.91 (m, 0.59 H, O-CH_2-O), 5.18-5.24 (m, 0.05 H, O-CH_2-O), 5.25-5.35 (m, 0.36 H, O-CH_2-O), 5.78 (s, 0.06 H, O-CH_2-O) ppm.

^{13}C APT-NMR spectroscopy (125 MHz, $CDCl_3$): δ = 20.7 (-, CH_3), 21.0 (-, CH_3), 55.9 (-), 55.9 (-), 79.2 (+, O-CH_2-O), 85.5 (+, O-CH_2-O), 86.9 (+, O-CH_2-O), 88.7 (+, O-CH_2-O), 88.8 (+, O-CH_2-O), 89.2 (+, O-CH_2-O), 90.2 (+, O-CH_2-O), 90.6 (+, O-CH_2-O), 92.4 (+, O-CH_2-O), 93.6 (+, O-CH_2-O), 93.7 (+, O-CH_2-O), 95.1 (+, O-CH_2-O), 169.7 (+, C=O), 170.4 (+, C=O) ppm.

IR spectroscopy: 3483 (b, vw, v[OH]), 2973 (w, v[CH_2]), 2911 (w, v[CH_2]), 1742 (m, v[C=O]), 1561 (w), 1466 (w), 1414 (w), 1369 (w), 1224 (m), 1197 (m), 1108 (m), 1005 (m), 915 (s), 834 (w), 606 (w), 535 (vw), 457 (vw) cm^{-1}.

ESI-MS spectroscopy (positive ions):
Series 1 (y=1): m/z(%) [x]= 387.12(1.91), 417.13(5.68), 447.14(10.92), 477.15(15.99), 507.16(16.49) [12], 537.17(14.79), 567.18(12.61), 597.19(9.29), 627.20(6.66), 657.22(3.70).
Series 2 (y=2): m/z(%) [x]= 371.09(0.54), 401.10(4.09), 431.11(7.48), 461.12(9.21), 491.13(11.20) [10], 521.14(9.41), 551.15(7.04), 581.16(5.02), 611.17(3.15), 641.18(2.36).
Series 3 (y=3): m/z(%) [x]= 385.10(2.70), 415.12(2.76), 445.13(19.66), 475.14(32.14), 505.15(69.63), 535.16(88.71) [10], 565.17(88.37), 595.18(70.16), 625.19(49.04), 655.20(31.31), 685.21(19.52), 715.22(11.29), 745.23(7.64), 775.24(3.60), 805.25(1.79).
Series 4 (y=2 $^{12}CO_2$ + 1 $^{13}CO_2$): m/z(%)= 416.12(0.52), 446.13(3.77), 476.14(6.02), 506.15(14.63), 536.16(20.15), 566.17(21.30) [11], 596.18(17.65), 656.20(9.88), 686.21(5.31), 716.22(3.13), 746.24(1.96), 776.25(1.30).
Series 5 (y=4): m/z(%) [x]= 429.13(1.43), 459.14(3.66), 489.15(6.40), 519.16(9.84), 549.17(11.91), 579.18(14.04), 609.19(14.36) [11], 639.20(13.66), 669.22(9.99), 729.24(6.32), 759.25(4.70).

Labelled $^{13}CO_2$-gas was used to elucidate the origin of the CO_2 that is incorporated into the polymer chain. The ESI-MS spectrum showed signals assigned to polymer chains with the same composition as product obtained with unlabelled CO_2. The chain containing three carbonate units and 10 FA-units prevailed. Polymer chains with one, two or four carbonate units were also present, but exhibited smaller intensities. Closer inspection of the ESI-MS spectra for chains, which contain labelled $^{13}CO_2$, revealed for instance series with two CO_2 and one $^{13}CO_2$. These series had the same intensity as for compound **H**. The ^{13}C NMR spectrum did not show a significant increase of the quaternary carbon signals at 169.7 ppm and 170.4 ppm compared to the compound **H**. A slightly more intense signal was observed in the 2D-NMR spectrum. Consequently, these results suggest that the incorporated CO_2 originates mainly from caesium carbonate.